

A Non-Linear Technique for MTPA-Based Induction Motor Drive Considering Iron Loss and Saturation Effects

Mohammad-Ali Salahmanesh
Faculty of Engineering
Ferdowsi University of Mashhad
Mashhad, Iran
m.salahmanesh@mail.um.ac.ir

Hossein Abootorabi Zarchi
Faculty of Engineering
Ferdowsi University of Mashhad
Mashhad, Iran
abootorabi@um.ac.ir

Hamidreza Mosaddegh Hesar
Faculty of Engineering
Ferdowsi University of Mashhad
Mashhad, Iran
h.mosaddegh@ferdowsi.um.ac.ir

Abstract— In this study, a novel maximum torque per ampere (MTPA) strategy based on backstepping controller is introduced for induction motor (IM) drives considering both iron loss and saturation effect. To achieve a perfect model for IM drives, inductances are accurately chosen in terms of magnetizing current by interpolating magnetizing flux curve. In addition, the MTPA strategy is performed with incorporating iron loss and saturation as major factors of current angle variations. In order to prove the stability of the control scheme, the Lyapunov control theory is used. By choosing both the MTPA realization criterion and rotor speed of IM as outputs, the proposed backstepping control converges the error signals to a small vicinity of zero. The simulation results are finally demonstrated to validate the proposed control structure.

Keywords— Induction motor (IM), backstepping control, maximum torque per ampere (MTPA), saturation effect, iron loss, field oriented control (FOC).

NOMENCLATURE

$\vec{i}, \vec{v}, \vec{\lambda}$	Current, Voltage, flux space vectors
\vec{i}_m, i_{mr}	Magnetizing and rotor magnetizing currents
T_e	Electromagnetic torque
R_s, R_r	Stator and rotor resistances
R_c	Iron loss resistance
L_{ls}, L_{lr}	Stator and rotor Leakage inductance
L_s, L_r	Self-inductance of the stator and rotor
L_m	Magnetizing inductance
T_s	Stator constant time
T'_s	Stator transient constant time
p	Number of pole pairs
ω_r	Electrical rotor speed
ω_s	Angular synchronous speed of the rotor flux
σ	Leakage factor ($1 - (L_m^2 / L_s L_r)$)
<i>Subscripts</i>	
s, r	Stator and rotor
D, Q	Stationary reference frame
d, q	Synchronously Rotating reference frame

I. INTRODUCTION

The induction motor (IM) has been widely utilized in various industrial applications due to its benefits such as long lifetime, low cost and high efficiency. Generally, the linear

magnetic models are adapted for analyzing the IMs. However, in some applications such as traction and field weakening, the IM usually needs to operate under the saturated conditions [1]. Likewise, the vector control performance is detuned with neglecting the iron loss and the saturation effects [2]. Thus, it is important to take their effects in the IM model and control schemes. There are two approaches to consider the saturation effects in the IM model. In first which is known as simplified model, the saturation effect is taken into account by substituting a non-linear function of magnetizing inductance into the voltage equations of the linear model [3]. The second approach is a full non-linear model in which the time variation of magnetizing inductance leads to different voltage equations in the full model and linear model. Therefore, the new terms arise as dynamic cross-saturation effects in the full model which is neglected in the simplified form [4]. Since, the full model is more accurate [5] and has faster response [6] in comparison to the simplified one, the full model of IMs is preferred in this paper. Regarding the nonlinear nature of the IMs and the wide range of their operation, a linear controller such as proportional-integral (PI) cannot perform properly [7]. Therefore, non-linear controllers such as sliding mode control [8], input-output feedback linearization (IOFL) [9,10] and backstepping control [11,12] have been presented to improve the performance of IM drives in the last decades. The feedback linearization (FL) often causes nonlinearities cancellation that can be useful for tracking. In contrast to FL, the backstepping control not only doesn't eliminate useful nonlinearities, but also defines extra nonlinear terms to have better transient performance. In the backstepping control design, the main purpose is to control the non-linear system in a recursive manner by choosing the state variables as "virtual controls" [13].

In this research work, a backstepping control is presented for IM drive which satisfies the maximum torque per ampere (MTPA) strategy. In this regard, the affine model of IM is modified to consider the iron loss and saturation effects. Moreover, the proposed MTPA developed according to Lagrange's Theorem determines optimal stator current angle.

Later in this paper, detailed description of the control system is introduced. In section II, the saturated model of IM is derived incorporating the iron loss. In section III, the principle of MTPA control strategy is proposed. In section IV, the backstepping controller is derived taking into consideration the magnetic saturation and iron loss. In this section the control laws are also obtained for IM drive. Finally, the simulation results and the concluding remarks are presented in sections V and VI, respectively.

II. IM MODEL INCLUDING IRON LOSS AND SATURATION EFFECTS

In the linear model of 3-phase IM, saturation effects are neglected and the all parameters such as stator and rotor self-inductances, as well as magnetizing inductance are considered constant. Tacking the magnetic saturation into account, the voltage equations differ from the equations obtained in their linear forms.

In the saturation condition, a dynamic inductance is introduced in addition to the static inductance which is equal to the derivative of flux-linkage space phasor with respect to the magnetizing-current space phasor. These inductances are calculated as follows:

$$L = \frac{d\lambda_m}{di_m}, \quad L_m = \frac{|\lambda_m|}{|i_m|} \quad (1)$$

where L and L_m are dynamic and static inductances, respectively. Since, these inductances are varied by time and the first-time derivative of magnetizing flux exists in the voltage equations, derivative of λ_m can be achieved in the stationary frame as follows:

$$\frac{d\lambda_{mD}}{dt} = L_{MD} \frac{di_{mD}}{dt} + L_{DQ} \frac{di_{mQ}}{dt} \quad (2)$$

$$\frac{d\lambda_{mQ}}{dt} = L_{MQ} \frac{di_{mQ}}{dt} + L_{DQ} \frac{di_{mD}}{dt} \quad (3)$$

In (2) and (3), L_{MD} and L_{MQ} are the direct and quadrature axis components of magnetizing inductance and L_{DQ} is the cross-coupling inductance which describes the magnetic influence of one axis on the other. These inductances are determined as follows:

$$L_{MD} = L \cos^2 \mu + L_m \sin^2 \mu \quad (4)$$

$$L_{MQ} = L \sin^2 \mu + L_m \cos^2 \mu \quad (5)$$

$$L_{DQ} = (L - L_m) \sin \mu \cos \mu \quad (6)$$

where μ is the angle of magnetizing current space vector defined as $i_m = |i_m|e^{j\mu}$. Under the linear magnetic condition, the dynamic inductance is equal to static inductance, because of the fact that the ratio of λ_m/i_m is constant. As a result, it can be concluded $L_{DQ} = 0$. $L_{mD} = L_{mQ}$. According to above equations, two axis model of IM in the stationary reference frame with considering the iron loss and magnetic saturation is obtained in the form:

$$\frac{R_c}{R_c + R_s} V_{sD} = (R_s \parallel R_c) i_{sD} + L_{sD} \frac{di_{sD}}{dt} + L_{mD} \frac{di_{mD}}{dt} + L_{DQ} \left(\frac{di_{sQ}}{dt} + \frac{di_{rQ}}{dt} \right) \quad (7)$$

$$\frac{R_c}{R_c + R_s} V_{sQ} = (R_s \parallel R_c) i_{sQ} + L_{sQ} \frac{di_{sQ}}{dt} + L_{mQ} \frac{di_{mQ}}{dt} + L_{DQ} \left(\frac{di_{sD}}{dt} + \frac{di_{rD}}{dt} \right) \quad (8)$$

$$0 = R_r i_{rD} + L_{rD} \frac{di_{rD}}{dt} + L_{mD} \frac{di_{sD}}{dt} + L_{DQ} \left(\frac{di_{sQ}}{dt} + \frac{di_{rQ}}{dt} \right) + \omega_r (L_r i_{rQ} + L_m i_{sQ}) \quad (9)$$

$$0 = R_r i_{rQ} + L_{rQ} \frac{di_{rQ}}{dt} + L_{mQ} \frac{di_{sQ}}{dt} + L_{DQ} \left(\frac{di_{sD}}{dt} + \frac{di_{rD}}{dt} \right) - \omega_r (L_r i_{rD} + L_m i_{sD}) \quad (10)$$

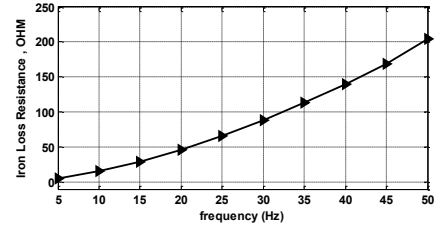


Fig.1. Measured Iron loss resistance in different frequencies for IM

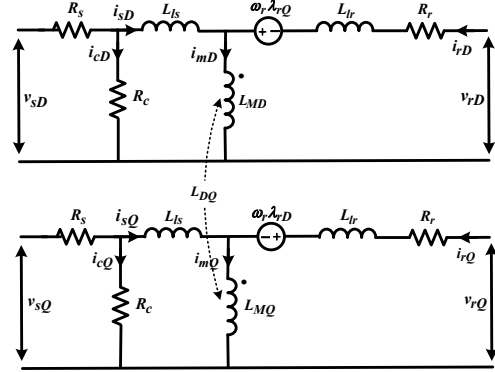


Fig.2. Equivalent circuit of an IM in the stationary reference frame including the iron loss and saturation effects

where $L_{sD,Q} = L_{ls} + L_{mD,Q}$ and $L_{rD,Q} = L_{lr} + L_{mD,Q}$ are self-inductances of stator and rotor windings, respectively. As shown in Fig. 1, the iron loss resistance is varied by power supply frequency. The equivalent circuit of IM with incorporating iron loss and saturation effects is also shown in Fig. 2. It can be observed from (7)-(10), the stator and rotor are coupled owing to cross-saturation and all inductances are modified in the saturated model. The saturation phenomenon doesn't add any extra term to unsaturated torque expression and it is therefore identical in the both saturation and linear condition. Consequently, it only effects on parameters such as magnetizing, rotor and stator inductances:

$$T_e = \frac{3p}{2} \frac{L_m}{L_r} (\lambda_{rD} i_{sQ} - \lambda_{rQ} i_{sD}) \quad (11)$$

The saturation of main flux path can be defined as a function of magnetizing current. In order to find the magnetizing curve, the no-load test is performed on a prototype IM [10]. The results are used to fit the magnetizing curve model as follows:

$$\lambda_m = 0.54365 - 0.55214 \cdot e^{-0.38127 \lambda_m^{1.84665}} \quad (12)$$

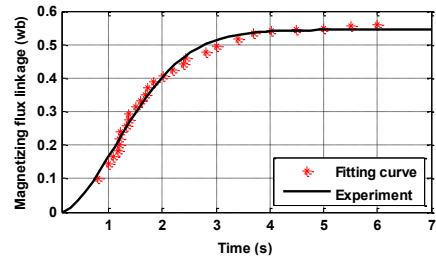


Fig. 3. Magnetizing curve

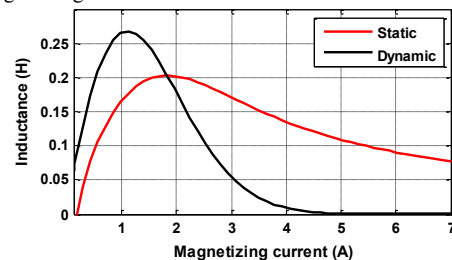


Fig.4. Static and dynamic inductances

Figures 3 and 4 show the magnetizing curve and the variations of L and L_m in terms of the magnetizing current, respectively. According to characteristic curve, the chord slope is equal to L_m and tangent slope in the operating point is equal to L . Considering (1), the static and dynamic inductances are obtained as follows:

$$L_m = \left(0.54365 - 0.55214 \cdot e^{-0.381275 i_m^{1.84665}} \right) / i_m \quad (13)$$

$$L = 0.38875 i_m^{0.84665} \cdot e^{-0.381275 i_m^{1.84665}} \quad (14)$$

In order to consider the saturation effect in controller design, the magnetizing inductance is defined as a function of the rotor magnetizing current (i_{mr}). In the rotor flux reference frame, the rotor magnetizing current is equal to the ratio of modulus of rotor flux-linkage space phasor to magnetizing inductance. Furthermore, the rotor magnetizing current only aligns with d-axis of the rotor flux-oriented reference frame. As a result, the voltage equations are simpler than those obtained from previous state. Due to the saturation, the extra terms Δi_{sd} and Δi_{sq} are added to equations under linear magnetic condition, as follows [14]:

$$T_s' \frac{di_{sd}}{dt} + i_{sd} = \frac{V_{sd}'}{(R_s \| R_c)} + \omega_s T_s' i_{sq} - (T_s - T_s') \frac{d|i_{mr}|}{dt} + \Delta i_{sd} \quad (15)$$

$$T_s' \frac{di_{sq}}{dt} + i_{sq} = \frac{V_{sq}'}{(R_s \| R_c)} - \omega_s T_s' i_{sd} - (T_s - T_s') \omega_s |i_{mr}| + \Delta i_{sq} \quad (16)$$

where $T_s' = \sigma L_s / (R_s \| R_c)$. As the rotor leakage inductance is negligible, Δi_{sd} and Δi_{sq} are derived as follows:

$$\Delta i_{sd} = \frac{L_m - L}{(R_s \| R_c)} \frac{d|i_{mr}|}{dt}, \quad \Delta i_{sq} = 0 \quad (17)$$

In contrast to the direct axis stator winding, there is not any additional induced electromotive force (emf) in quadrature axis stator winding. The rotor flux-oriented reference frame is achieved as:

$$\lambda_{rd} = |\lambda_r|, \quad \lambda_{rq} = 0 \quad (18)$$

Due to the rotor flux-oriented reference frame, the equations of the IM taking into account the saturation effects and iron loss are written in the form of affine as follows:

$$\dot{X} = f(x) + g_1(x)v_{ds}' + g_2(x)v_{qs}' \quad (19)$$

where

$$f(x) = \begin{bmatrix} \frac{-(R_s \| R_c)}{\sigma L_s} x_1 + \omega_s x_2 + \frac{R_r L_m}{\sigma L_s L_r L} \left(\frac{-L_m^2}{L_r} + L_m - L \right) (x_1 - x_3) \\ \frac{-(R_s \| R_c)}{\sigma L_s} x_2 - \omega_s x_1 - \frac{L_m^2}{\sigma L_s L_r} \omega_s x_3 \\ \frac{R_r L_m}{L_r L} (x_1 - x_3) \\ \frac{T_e}{j} - \frac{T_l}{j} - \frac{B}{j} x_4 \end{bmatrix}$$

$$g_1(x) = \begin{bmatrix} \frac{1}{\sigma L_s} \\ 0 \\ 0 \\ 0 \end{bmatrix}, \quad g_2(x) = \begin{bmatrix} 0 \\ 1 \\ \sigma L_s \\ 0 \end{bmatrix}$$

with

$$x = [i_{sd} \quad i_{sq} \quad i_{mr} \quad \omega_r] , \quad V_{sd}' = \frac{R_c}{R_c + R_s} V_{sd}, \quad V_{sq}' = \frac{R_c}{R_c + R_s} V_{sq}$$

III. PROPOSED MTPA STRATEGY

Minimization of IM stator current is considered as one of the control objectives. According to Lagrange's theorem, the proposed MTPA will realize when the stator current curve and the torque curve are tangent at a point if and only if their gradient vectors are parallel, so that:

$$\|\nabla T_e(i_{sd}, i_{sq})\| \|\nabla I_s^2(i_{sd}, i_{sq})\| \sin \alpha = 0 \quad (20)$$

The magnitude of cross-product of $\nabla T_e(i_{sd}, i_{sq})$ and $\nabla I_s^2(i_{sd}, i_{sq})$ and rotor speed are chosen as control outputs, and output vector $Y = [y_1 \quad y_2]^T$ is introduced as (21) and (22) to attain the control objectives [15]:

$$y_1 = \|\nabla T_e(i_{sd}, i_{sq})\| \|\nabla I_s^2(i_{sd}, i_{sq})\| \sin \alpha = \det \begin{bmatrix} \frac{\partial T_e}{\partial i_{sd}} & \frac{\partial T_e}{\partial i_{sq}} \\ \frac{\partial I_s^2}{\partial i_{sd}} & \frac{\partial I_s^2}{\partial i_{sq}} \end{bmatrix} \quad (21)$$

$$y_2 = \frac{1}{j} (T_e - T_l) = \frac{1}{j} \left(\frac{\beta^2 - 1}{\beta^2 + 1} \right) \cdot \left(\frac{R_l}{\beta \omega} \right) \left(i_{sq} i_{sd} - \frac{i_{sq}^2}{\beta} \right) - \frac{T_l}{j} \quad (22)$$

where $\beta = \frac{R_c}{\omega_s L_r} + \frac{R_c}{\omega_s L_m}$. If y_1 keeps at zero, the proposed

MTPA will realize obviously. By accomplishing some calculations on y_1 , we have:

$$i_{sq} = \pm i_{sd} \xi \quad (23)$$

where $\xi = \left(\left(\sqrt{\beta^2 + 1} - 1 \right) / \beta \right)$. The variation of ξ versus frequency has been plotted in Fig. 5.

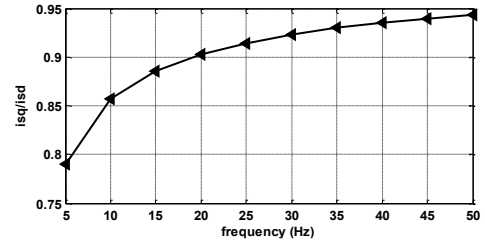


Fig.5. variation of ξ versus frequency

IV. BACKSTEPPING CONTROL FOR IM

In the non-linear control design, the control objectives are realization of MTPA strategy and the rotor speed tracking. In this way, the tracking errors are defined as follows:

$$e_1 = y_1 - y_{1ref} \quad (24)$$

$$e_2 = y_2 - y_{2ref}$$

where $y_1 = x_2 - \xi x_1$ and $y_2 = x_4$ depend on the MTPA strategy and the rotor speed respectively. According to MTPA realization criterion $y_{2ref} = 0$, the error dynamics are obtained as:

$$\dot{e}_1 = \dot{x}_2 - \xi \dot{x}_1 \quad (25)$$

$$\dot{e}_2 = \dot{x}_4 - \dot{x}_{4ref}$$

The error dynamics can be rewritten by lie derivatives:

$$\begin{bmatrix} \dot{e}_1 \\ \dot{e}_2 \end{bmatrix} = \begin{bmatrix} L_f e_1 \\ L_f e_2 \end{bmatrix} + \begin{bmatrix} L_g e_1 & L_g e_2 \end{bmatrix} \begin{bmatrix} v_{ds}' \\ v_{qs}' \end{bmatrix} - \begin{bmatrix} 0 \\ \dot{x}_{4ref} \end{bmatrix} \quad (26)$$

where $L_f y_i$ ($i = 1, 2, \dots$) are defined as the lie derivative of output function $y(x): \mathbb{R}^n \rightarrow \mathbb{R}$ along a vector field $f(x) = (f_1(x), \dots, f_n(x))$:

$$L_f y(x) = \sum_{i=1}^n \frac{\partial y}{\partial x_i} f_i(x) \quad (27)$$

The lie derivative functions of the first tracking error are computed as:

$$L_f e_1 = -\xi \left(\frac{-(R_s \| R_c)}{\sigma L_s} x_1 + \omega_3 x_2 + \frac{R_r L_m}{\sigma L_s L_r L} \left(\frac{-L_m^2}{L_r} + L_m - L \right) (x_1 - x_3) \right) + \left(\frac{-(R_s \| R_c)}{\sigma L_s} x_2 - \omega_3 x_1 - \frac{L_m^2}{\sigma L_s L_r} \omega_3 x_3 \right) \quad (28)$$

$$L_{g_1} e_1 = -\xi \left(\frac{1}{\sigma L_s} \right), \quad L_{g_2} e_1 = \left(\frac{1}{\sigma L_s} \right) \quad (29)$$

The electromagnetic torque in the rotor flux-oriented control is expressed as:

$$T_e = \frac{3P L_m^2}{2 L_r} (x_3 x_2) \quad (30)$$

By substituting (30) into the speed mechanical equation, the lie derivative functions of the second tracking error are computed as:

$$L_f e_2 = \frac{3P L_m^2}{2j L_r} x_3 x_2 - \frac{T_L}{j} - \frac{B}{j} \omega_r \quad (31)$$

$$L_{g_1} e_2 = 0, \quad L_{g_2} e_2 = 0 \quad (32)$$

Since, the input voltages (V'_{sd}, V'_{sq}) don't appear in the second dynamic, $x_3 x_2$ is chosen as the virtual control to converge e_2 to zero. Now, we introduce the Lyapunov function as $V_1 = 1/2(e_1^2 + e_2^2)$, hence the first time derivative of V_1 is:

$$\dot{V}_1 = -\alpha e_1^2 - \beta e_2^2 \quad (33)$$

where α and β are positive design gains. According to (33), the stabilization virtual function and first input control law are constructed as:

$$(x_3 x_2)_{ref} = \frac{2L_r}{3PL_m^2} (T_l + B \omega_r + j \dot{\omega}_{ref} - j \beta e_2) \quad (34)$$

$$(L_{g_1} e_1 V'_{ds} + L_{g_2} e_2 V'_{qs})_{ref} = -L_f e_1 - \alpha e_1 \quad (35)$$

The next step tries to make $x_3 x_2$ equal to as desired value obtained in (34). Thus, the third error signal is defined as $e_3 = x_3 x_2 - (x_3 x_2)_{ref}$. According to the equations (24)-(35), the error dynamics can be rewritten as follows:

$$\dot{e}_1 = -\alpha e_1 \quad (36)$$

$$\dot{e}_2 = -\beta e_2 + \frac{3P L_m^2}{2 L_r} j e_3 \quad (37)$$

$$\dot{e}_3 = L_f e_3 + L_{g_1} e_1 V'_{ds} + L_{g_2} e_2 V'_{qs} - \frac{d(x_3 x_2)_{ref}}{dt} \quad (38)$$

where

$$L_f e_3 = x_3 \left(\frac{-(R_s \| R_c)}{\sigma L_s} x_1 + \omega_3 x_2 + \frac{R_r L_m}{\sigma L_s L_r L} \left(\frac{-L_m^2}{L_r} + L_m - L \right) (x_1 - x_3) \right) + x_2 \left(\frac{R_r L_m}{L_r L} (x_1 - x_3) \right) \quad (39)$$

$$L_{g_1} e_3 = 0, \quad L_{g_2} e_3 = x_3 \frac{1}{\sigma L_s} \quad (40)$$

$$\frac{d(x_3 x_2)_{ref}}{dt} = \frac{2L_r}{3PL_m^2} (\dot{T}_l + B \dot{\omega}_r + j \dot{\omega}_{ref} - j \beta \dot{e}_2) \quad (41)$$

As the actual control input V'_{qs} is observed in new dynamic \dot{e}_3 , a new Lyapunov function is selected as $V_2 = 1/2(e_1^2 + e_2^2 + e_3^2)$ to design the final control law. Taking the first time derivative of this function \dot{V}_2 and replacing the error dynamics (36)-(38), \dot{V}_2 can be computed as follows:

$$\dot{V}_2 = e_1 (-\alpha e_1) + e_2 \left(-\beta e_2 + \frac{3P L_m^2}{2 L_r} j e_3 \right) + \quad (42)$$

$$e_3 \left(L_f e_3 + L_{g_2} e_2 V'_{qs} - \frac{d(x_3 x_2)_{ref}}{dt} \pm \gamma e_3 \right)$$

The time derivative V_2 can be also obtained as $\dot{V}_2 = -\alpha e_1^2 - \beta e_2^2 - \gamma e_3^2$ if the control laws are determined as follows:

$$V'_{qs} = \frac{1}{L_{g_2} e_2} \left(-\frac{3P L_m^2}{2 L_r} j e_2 - L_f e_3 + \frac{d(x_3 x_2)_{ref}}{dt} - \gamma e_3 \right) \quad (43)$$

$$V'_{ds} = \frac{1}{L_{g_1} e_1} (-L_f e_1 - \alpha e_1 - L_{g_2} e_2 V'_{qs}) \quad (44)$$

The MTPA realization criterion and the tracking of the rotor speed reference are satisfied for α, β and $\gamma > 0$,

V. SIMULATION RESULTS

In order to assess the performance of proposed control technique, simulations are fulfilled in MATLAB/SIMULINK[®] environment. The specifications of the simulated motor are given in Table I. The overall structure of IM drives is shown in Fig. 6. Also, the simulation results for rotor speed control and realization of MTPA strategy are illustrated in Figs 7-14 with considering iron loss and saturation effects. Fig. 7 shows the rotor speed response of the proposed drive and its reference. The speed reference is stepped up at time intervals 0-2s and 4-6s. Then it is stepped down to 40 rad/sec at t=10s. As can be obviously seen, the rotor speed follows its reference smoothly in both transient and steady state condition. According to speed transient periods, the electromagnetic torque increases and decreases as a step change, which is presented in Fig. 8. The static and the dynamic inductances are shown in Fig. 9. As observed, these inductances are achieved from the magnetizing curve, and are modified with operating points.

Figure 10 shows variations of MTPA factor with respect to frequency, which is computed by (23). So, as illustrated in Fig. 5, the MTPA factor is continuously changed by varying rotor speed command. Although, in ideal condition this factor is equal to one, it is smaller than one when the iron loss and saturation effects are taken into account. Considering the MTPA factor, d-axis component isn't identical to q-axis component of the stator current in the rotor flux-oriented reference frame (Fig. 11). According to Fig. 12, the MTPA realization criterion tracks its reference value, which is zero, and the MTPA strategy is, therefore, satisfied. The d and q-axis components of rotor flux and the d-axis stator current component in both saturation and linear models are illustrated in Figs 13 and 14, respectively. As depicted in Fig. 14, since the static and dynamic inductances are time varying in the saturated model, the amplitude of D-axis stator current component is different from the linear one, during open-loop test. In this test, the voltage of power supply is 180 V_{rms} .

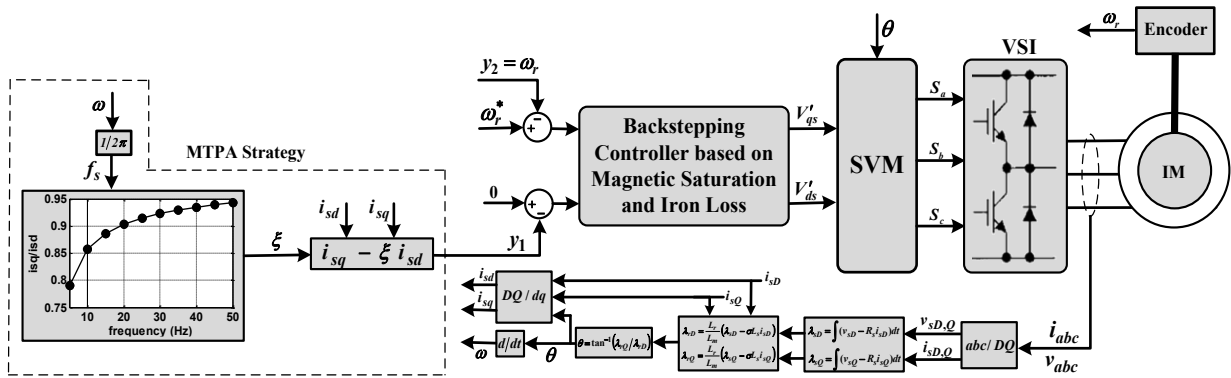


Fig. 6. The block diagram of MTPA strategy for backstepping control based IM drive

TABLE I: THE IM PARAMETERS [10]

Parameter	Value	Parameter	Value
Pole-Pair	2	R'_r (Ω)	1.1237
Rated torque (N.m)	10	L_{ls} (H)	0.047
Rated voltage (v)	180 (L-L)	L'_{lr} (H)	0.0206
R_s (Ω)	1.3012	L_m (H)	0.1863

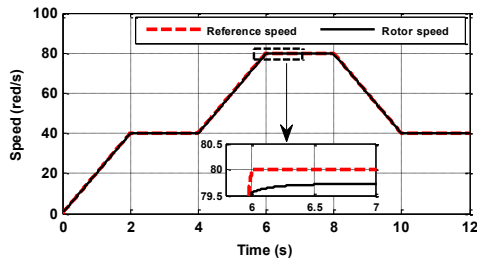


Fig. 7. Rotor speed response of the non-linear controller

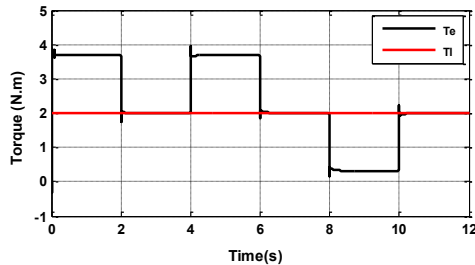


Fig. 8. Electromagnetic and load torques

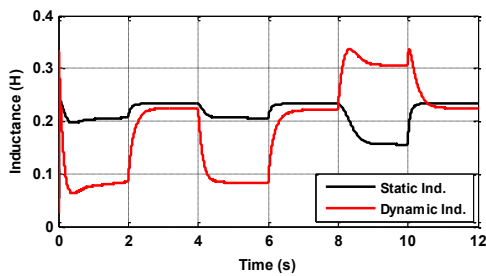


Fig. 9. static and Dynamic inductances

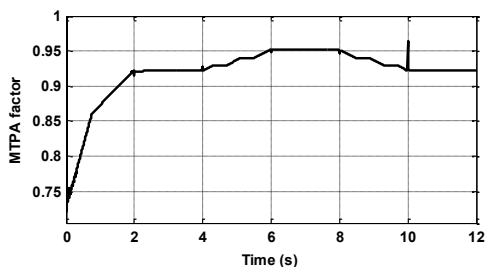


Fig. 10. Variation of MTPA factor by changing rotor speed reference

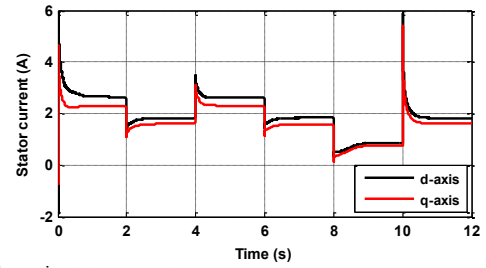


Fig. 11. d-q axis stator currents

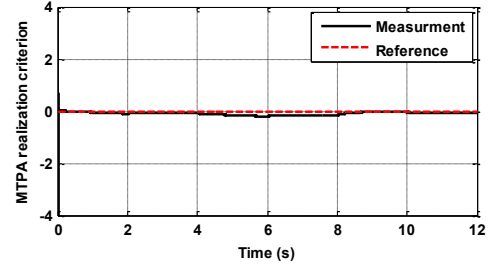


Fig. 12. MTPA realization criterion

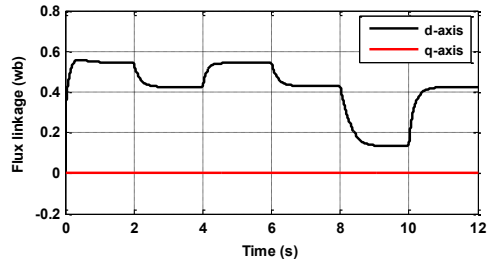


Fig. 13. d-q axis rotor flux components

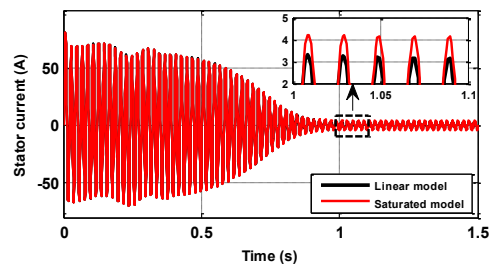


Fig. 14. D-axis component of stator current for open-loop condition

VI. CONCLUSION

In this paper, a direct field-oriented control method based on backstepping controller is introduced for three-phase IM drives incorporating iron loss and magnetic saturation. In this regard the affine IM model is derived and the reference voltages are determined according to the control laws. It is noteworthy that the state variables in the saturated IM model is increased due to the iron loss consideration. This makes the derivation of the nonlinear controller more complex.

Therefore, there has not been much effort to take the effects of the iron loss in the backstepping-based FOC into account. In order to achieve the maximum torque per stator current, a realization criterion is also derived based on Lagrange's Theorem. The simulation results verified the effectiveness and capability of the proposed method.

REFERENCES

- [1] L. Liu, X. Du, and S. Shen, "Indirect Field-Oriented Torque Control of Induction Motor Considering Magnetic Saturation Effect: Error Analysis," *IET Electr. Power Appl.*, vol. 11, no. 6, pp. 1105–1113, 2017.
- [2] E. Levi, S. Vukosavic, and V. Vuckovic, "Saturation Compensation Schemes for Vector Controlled Induction Motor Drives," in *Conf. Rec. IEEE Power Elect. Specialists Conf.*, pp. 591–598, 1990.
- [3] Y. Zeng, M. Cheng, X. Wei, and L. Xu, "Dynamic Modeling and Performance Analysis with Iron Saturation for Dual-Stator Brushless Doubly Fed Induction Generator," *IEEE Trans. Energy Convers.*, DOI: 10.1109/TEC.2019.2942379.
- [4] A. Accetta, F. Alonge, M. Cirrincione, M. Pucci, and A. Sferlazza, "Feedback Linearizing Control of Induction Motor Considering Magnetic Saturation Effects," *IEEE Trans. Ind. Appl.*, vol. 52, no. 6, pp. 4843–4854, 2016.
- [5] P. Vas, "Generalized Analysis of Saturated AC Machines," vol. 64, pp. 57–62, 1981.
- [6] O. Kiselychnyk, M. Bodson, and J. Wang, "Comparison of Two Magnetic Saturation Models of Induction Machines and Experimental Validation," *IEEE Trans. Ind. Electron.*, vol. 64, no. 1, pp. 81–90, 2017.
- [7] W. Li and J. Slotine, *Applied Nonlinear Control*, Englewood Cliffs, NJ: Prentice-Hall, 1991.
- [8] M. Comanescu, L. Xu, and T. D. Batzel, "Decoupled Current Control of Sensorless Induction-Motor Drives by Integral Sliding Mode", *IEEE Trans. Ind. Electron.*, vol. 55, no. 11, pp. 3836-3845, November 2008.
- [9] C. Lascu, S. Jafarzadeh, S. M. Fadali, and F. Blaabjerg, "Direct Torque Control with Feedback Linearization for Induction Motor Drives," *IEEE Trans. Power Electron.*, vol. 32, no. 3, pp. 2072-2080, March 2017.
- [10] M. A. Salahmanesh, H. A. Zarchi, and H. M. Hesar, "Lyapunov - Based Input-Output Feedback Linearization Control of Induction Motor drives Considering Online MTPA Strategy and Iron Loss," *ICEE 2019 - 27th Iran. Conf. Electr. Eng.*, pp. 697–701, 2019.
- [11] M. Hajian, J. Soltani, G. A. Markadeh, and S. Hosseinnia, "Adaptive Nonlinear Direct Torque Control of Sensorless IM Drives with Efficiency Optimization," *IEEE Trans. Ind. Electron.*, vol. 57, no. 3, pp. 975–985, 2010.
- [12] M. N. Uddin, and S. W. Nam, "Development and Implementation of a Nonlinear-Controller-Based IM Drive Incorporating Iron Loss with Parameter Uncertainties," *IEEE Trans. Ind. Electron.*, vol. 56, no. 4, pp. 1263–1272, 2009.
- [13] M. Krstic, I. Kanellakopoulos, and P. Kokotovic, *Nonlinear and Adaptive Control Design*. New York: Wiley, 1995.
- [14] P. Vas, *Sensorless Vector and Direct Torque Control*, Oxford University Press, 1998.
- [15] H. Mosaddegh Hesar, H. Abootorabi Zarchi, and M. Ayaz Khoshhava, "Online Maximum Torque per Ampere Control for Induction Motor Drives Considering Iron Loss Using Input-Output Feedback Linearisation", *IET Electr. Power Appl.*, vol. 13, no. 12, pp. 2113-2120, December 2019.